Supplementary Information for "Tuning a magnetic energy scale with pressure and field in UTe_2"

Hyunsoo Kim,[1,2] I-Lin Liu,[2] Wen-Chen Lin,[2] Yun Suk Eo,[2]
Sheng Ran,[2] Nicholas P. Butch,[2,3] and Johnpierre Paglione[2,4]

[1] *Department of Physics, Missouri University of Science and Technology, Rolla, MO 65409, USA*

[2] *Maryland Quantum Materials Center and Department of Physics, University of Maryland, College Park, Maryland, USA*

[3] *NIST Center for Neutron Research, National Institute of Standards and Technology, Gaithersburg, MD 20899, USA*

[4] *Canadian Institute for Advanced Research, Toronto, Ontario M5G 1Z8, Canada*

Corresponding authors:
Johnpierre Paglione (paglione@umd.edu),
Hyunsoo Kim (hyunsoo.kim@mst.edu)

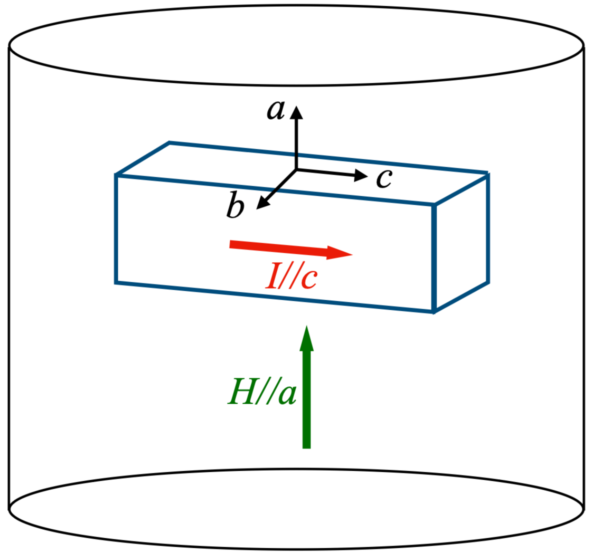

Supplementary Figure 1. Illustration of sample orientation (blue cuboid) with respect to the electrical current I (red) and magnetic field H (green) in a inner volume of a piston clamp pressure cell, represented by a cylinder.

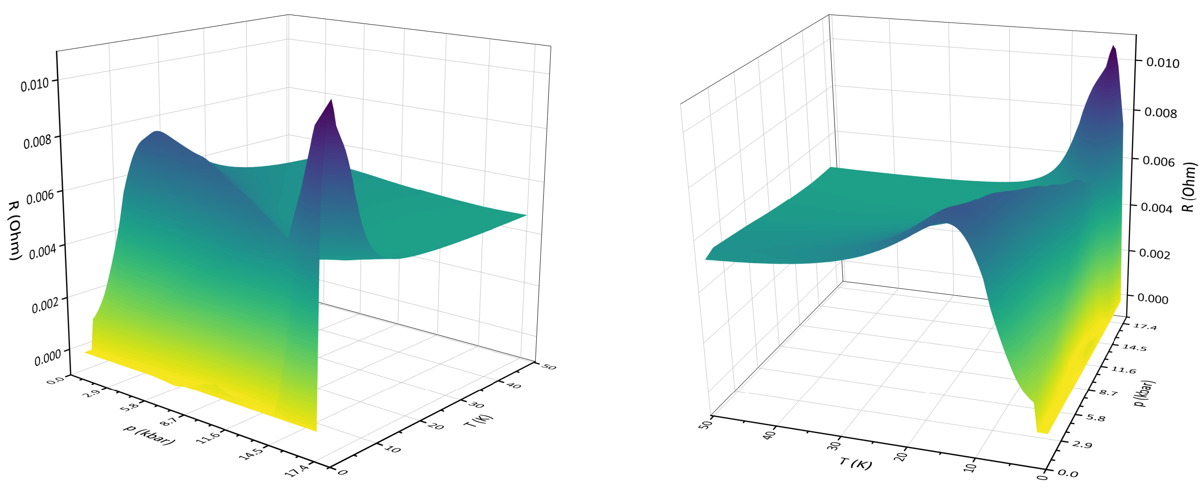

Supplementary Figure 2. 3D surface plots of $R(T,p)$ in UTe_2 with the electric current along the c-axis in two different viewing perspectives.

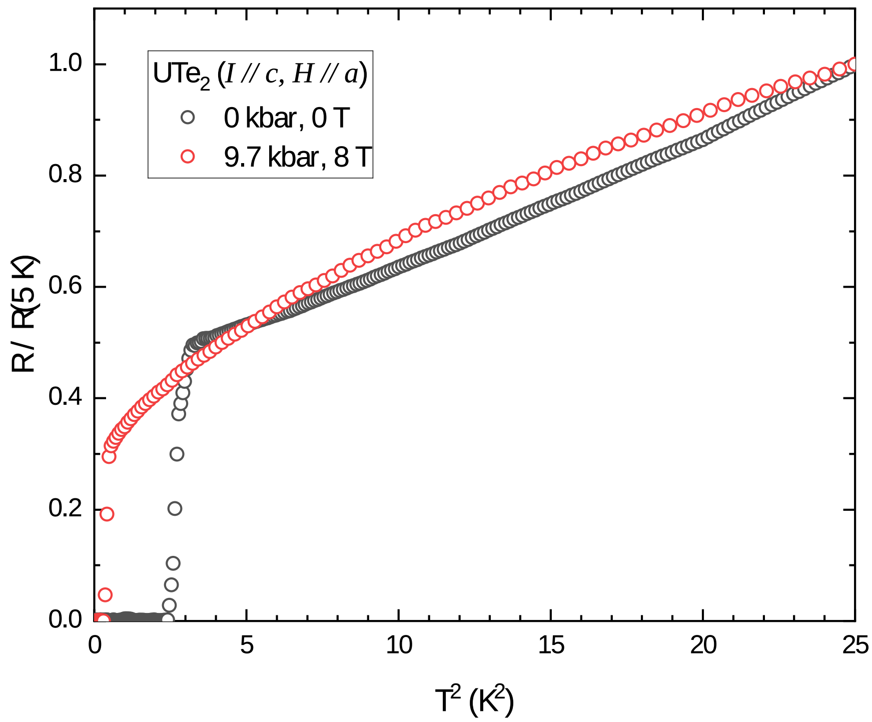

Supplementary Figure 3. Comparison of the power-law behavior in UT_2 with $I \parallel c$ and $H \parallel a$. The Fermi liquid behavior T^2 at ambient pressure and zero magnetic field becomes nearly linear resistivity in temperature under 9.7 kbar and 8 T (see main text for details).

$\mu_0 H$ [T]	5.3 kbar	7.5 kbar	9.7 kbar	11.8 kbar	14.2 kbar
0	10.5	8.3	6.99	4.34	
2	11	9	6.99	4.74	
4	11.5	9.5	7.59	5.59	
6	12.5	10.5	8.58	6.76	5.1
8	13.5	11.5	9.8	8.17	6.8
10	15	13	11.2	9.78	8.6
12	16	14.5	12.6	11.19	10.2
14	17.5	15.5	14	12.88	11.8
16	18.5	17	15.4	14.2	13.4
18	19.5	18	16.6	15.68	14.8

Supplementary Table 1. Field- and pressure-dependent c-axis peak position T^* presented in Fig. 2 in the main text. The temperature values are presented in Kelvin.

p [kbar]	T_c [K]	$\mu_0 dH_{c2}/dT$ [T/K]	$\mu_0 H_{c2}(0)$ [T]	$\mu_0 H_{HW}$ [T]	$\mu_0 H_P$ [T]
0	1.56	-6.25	6.3 ± 0.5	6.9 ± 0.2	2.9
5.3	2.24	-7.38	8.7 ± 1.1	11.7 ± 0.3	4.2
7.5	2.78	-9.72	10.6 ± 0.8	19.2 ± 0.5	5.2
9.7	2.85	-25.0	10.0 ± 0.5	51.0 ± 1.4	5.3
11.8	2.75	-20.0	8.8 ± 0.5	39.1 ± 1.1	5.1
14.2	1.65			7.8 ± 0.3	3.1

Supplementary Table 2. The superconducting critical temperature and upper critical fields. $H_{c2}(0)$ is determined from experimental values by extrapolating to $T = 0$, and H_{HW} and H_P are theoretical estimates, see main text for details.

$\mu_0 H$ [T]	5.3 kbar	7.5 kbar	9.7 kbar	11.8 kbar	14.2 kbar
0	1.95 ± 0.10	2.17 ± 0.33			
2	1.89 ± 0.07	2.84 ± 0.26	2.49 ± 0.58		
4	1.76 ± 0.02	1.75 ± 0.04	1.24 ± 0.11		
6	1.58 ± 0.01	1.29 ± 0.02	1.08 ± 0.02	1.37 ± 0.20	
8	1.57 ± 0.01	1.26 ± 0.01	1.18 ± 0.01	1.23 ± 0.02	1.54 ± 0.03
10	1.46 ± 0.01	1.32 ± 0.01	1.40 ± 0.01	1.61 ± 0.02	1.98 ± 0.01
12	1.46 ± 0.01	1.45 ± 0.01	1.57 ± 0.01	1.84 ± 0.01	2.23 ± 0.01
14	1.49 ± 0.01	1.58 ± 0.01	1.73 ± 0.01	2.02 ± 0.01	2.39 ± 0.01
16	1.55 ± 0.01	1.65 ± 0.01	1.84 ± 0.01	2.15 ± 0.01	2.48 ± 0.01
18	1.67 ± 0.01	1.75 ± 0.01	1.94 ± 0.01	2.28 ± 0.01	2.55 ± 0.01

Supplementary Table 3. Power-law exponent n determined from the least square fitting of AT^n with temperatures up to $T^*/2$. The coefficient A is presented in Supplementary Table 4.

$\mu_0 H$ [T]	5.3 kbar	7.5 kbar	9.7 kbar	11.8 kbar	14.2 kbar
0	107.0 ± 21.9	88.1 ± 52.6			
2	119.0 ± 17.0	31.0 ± 13.9	63.8 ± 59.4		
4	142.7 ± 4.9	175.1 ± 11.9	527.0 ± 121.9		
6	190.7 ± 4.9	424.6 ± 15.4	747.7 ± 37.6	533.7 ± 168.4	
8	164.7 ± 4.8	389.8 ± 10.9	494.6 ± 10.1	499.6 ± 16.0	370.8 ± 14.8
10	186.0 ± 4.4	273.0 ± 6.1	249.5 ± 5.7	196.7 ± 4.9	116.0 ± 2.4
12	153.3 ± 3.1	166.4 ± 3.8	141.2 ± 3.7	94.0 ± 2.2	50.0 ± 0.8
14	122.4 ± 2.2	105.3 ± 2.3	82.6 ± 1.8	49.8 ± 1.1	25.5 ± 0.5
16	89.6 ± 1.8	75.9 ± 1.6	52.7 ± 1.0	29.3 ± 0.5	15.4 ± 0.3
18	59.1 ± 1.2	52.0 ± 0.9	35.4 ± 0.5	18.0 ± 0.3	10.1 ± 0.2

Supplementary Table 4. The power-law coefficient A in $\mu\Omega/\mathrm{K}^n$ from least square fitting of power-law where n values are presented in Supplementary Table 3.